

# Single-phase conjugate heat transfer analysis of U-bend microchannel (UBMC) and compare the result with a Straight microchannel (SMC) of same length

RAVI RANJAN KUMAR

M.Tech. Student NIT Rourkela  
Department of Mechanical Engineering,  
National Institute of Technology Rourkela, Rourkela-769008, India

**Abstract:** Single-phase conjugate heat transfer analysis of U-bend microchannel (UBMC) a three –dimensional numerical study for laminar flow has been performed to evaluate the fluid flow and heat transfer characteristics. Three different geometry configurations are considered for the UBMC with a constant hydraulic diameter of 0.4 mm and radius of curvature of the U bend  $R = 2$  mm, 3 mm, and 4 mm. Comparison of UBMC is done with equivalent length (along center) straight microchannel (SMC) with total channel length  $L = 36.2$  mm, 39.4 mm, and 42.5 mm, respectively, for three different Reynolds numbers of 50, 100, and 200 at a constant applied heat flux of  $49184$  W/m<sup>2</sup>. The performance evaluation factor (PEF) value indicate an improvement in heat transfer rate for the UBMC compared to SMC. Parameters such as the local Nusselt number, average Nusselt number, and total pressure drop are evaluated. It is observed that bending effect improved overall performance of UBMC over SMC by 34% for  $R = 4$  mm at a Reynolds number of 200. Qualitative picture of the impact of curvature on the performance of UBMC in the form of velocity and temperature contours are also presented. It is also found that performance of UBMC with low radius of curvature can be improved with high pumping power, since the pressure drop is unavoidable. So, it is better to use channels with high radii of curvature at relatively low Reynolds number.

**Keywords:** Heat flux, Average Nusselt number, Total pressure drop, Performance evaluation factor.

## 1. INTRODUCTION

Microchannel is a channel with a hydraulic diameter below 1 mm is used in fluid control and heat transfer. They are more efficient than macro counterparts because of a high surface-area to volume ratio yet pose a multitude of challenges due to their small size. There is a constant demand for high heat flux removal from miniaturized electronic devices for better performance and life. Enhancement of the heat transfer process is directly dependent upon the surface area as it occurs across the channel walls. As the diameter of the channel decreases, the surface area to the volume ratio increases leading to efficient transport processes and lower coolant requirements than conventional-sized channels. Therefore, there is a need for a miniaturized channel to intensify the rate of heat transfer. Researchers have found different microchannel-based cooling methods that have their advantages and limitations.

**Application-** (i) Electronic cooling system (ii) cooling of microchips (iii) Heat exchangers application.

## 2. LITERATURE REVIEW AND OBJECTIVE

Tuckerman and Pease, who studied the thermo-hydrodynamics of forced convective heat transfer through a simple and straight microchannel, many passive and active enhancement techniques have been developed to cater to the high heat flux dissipation requirement. These include introducing roughness structures in channel walls, flow disruptions, channel curvature, fluid additives, electrostatic field, flow pulsation, etc. The design modifications improved the wall average Nusselt number  $Nu$  and friction factor  $f$ . As demonstrated by Sturgis and Mudawar for a hydraulic diameter of 3.33 mm, heat transfer enhancement in a curved channel resulted in a 26% improvement compared to the straight channel. But this range was within the conventional size limit. There is an added advantage for the microscale range where the radius of curvature is most practically achievable compared to the conventional-sized channels. Pradhan et al. studied the heat transfer characteristics of a conventional U-bend pipe of different cross sections. They found the highest heat transfer rate for the non-circular cross sections compared to the circular ones. Nivedita et al. investigated the dean flow in microchannels experimentally and numerically and observed the presence of secondary Dean Vortices that create secondary flows in curvilinear geometry. Zhang et al. performed multi-objective optimization considering three different parameters maximum temperature, thermal resistance, and pressure drop. For optimization purposes, both the thermal resistance and pressure drop should be taken into account. Neama et al. did numerical and experimental investigation of

a flow-through serpentine microchannel with single, double, and triple paths. The single path channel provided the best heat transfer performance followed by double and triple paths. This paper uses a computational method to analyze heat transfer through a 180° U-bend microchannel with a rectangular cross-section.

**COMPUTATIONAL METHOD**

**2.1 Problem description.**

**Table-1**

Parameters in (mm)	L	$W_s$	$W_f$	$\delta_f$	$\delta_s$	R
SMC	36.2, 39.4, 42.5	0.8	0.4	0.4	0.4	-
UMC	-	0.8	0.4	0.4	0.4	2, 3, 4

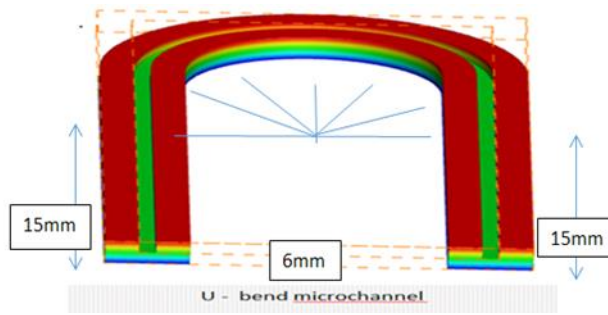


Figure - 1 Geometry

- Width of solid domain ( $W_s$ ) = 0.8mm
- Width of fluid domain ( $W_f$ ) = 0.4 mm
- Depth of fluid domain = 0.4 mm
- Depth of solid domain = 0.4mm

Here all case both vertical height is 15 mm only change radius of curvature length. For  $Re = 50$  three case  $R=2mm$ ,  $R=3mm$  and  $R=4mm$ , for  $Re = 100$  three case  $R=2mm$ ,  $R=3mm$  and  $R=4mm$ , for  $Re = 200$  ,  $R = 2mm$ ,  $R = 3mm$  and  $R = 3mm$

THE MODELLING SIMPLIFIES BY THE FOLLOWING ASSUMPTIONS

(i) steady state laminar flow, (ii) single phase and incompressible, (iii) thermophysical properties are constant for both solid and liquid, (iv) no internal heat generation, (v) no viscous dissipation. The governing equation is as follows:

**equations:-**

- (i) Continuity equation:  
 $\nabla \cdot V = 0$
- (ii) Momentum equations:  
 $\rho [\partial V / \partial t + (\nabla \cdot V)^2] = -\nabla p + \mu \nabla^2 V$
- (iii) Energy equation:  
 $\rho f c_f [\partial T / \partial t + V \cdot \nabla T] = \nabla \cdot k_f$
- (iv) Energy equation for the solid,  
 $\nabla^2 T_s = 0$

**BOUNDARY CONDITION**

Constant heat flux boundary condition is applied at the bottom, where  $q = 47000 W/m^2$ , and  $q = 0$  on the other walls including side walls. Water is used as a coolant and aluminium as the substrate material. The thermophysical properties of water and aluminium are listed in Table. 2

**Table 2: Thermophysical properties of the coolant and substrate material at 300K**

<u>Material</u>	$\rho(kg/m^3)$	$k(W/mK)$	$C_p(\frac{J}{kg \cdot K})$	$\mu(\frac{kg}{ms})$
<u>Aluminium</u>	2719	237	871	-
<u>Water</u>	998.2	0.6	4182	0.001003

## 2.2 Method of calculation

Finite volume-based commercially available CFD solver ANSYS Fluent V20 is used for solving the governing differential equations. The SIMPLE algorithm is used for pressure-velocity coupling. Second order upwind is used to discretize the momentum and energy equations. The residual levels for convergence were taken as  $10^{-6}$ ,  $10^{-6}$  and  $10^{-8}$  for continuity equation, momentum equations and energy equation respectively.

## 2.3 DATA ACQUISITION

Various parameters that will help us evaluate the (PEF)

Local Nusselt number,

$$Nu_z = \frac{h_z \cdot D_h}{k_f}$$

Local heat transfer coefficient,|

$$h_z = \frac{q_z}{(T_w - T_f)}$$

Average Nusselt Number,

$$Nu_{avg} = \frac{1}{L} \int_0^L Nu_z dz$$

Thermal Resistance

$$R_{th} = \frac{T_{max} - T_{min}}{Q}$$

Performance Evaluation Factor,

$$PEF = \frac{Nu_{avg}/Nu_o}{(\Delta p/\Delta p_o)^{\frac{1}{2}}}$$

## 2.4 Grid Independence study

We know that if very fine mesh that is large mesh size is consider then time taken to coverge the solution is more but accurse is more but if small mess size is consider then time taken to converge the solution is less but accuracy is less Grid Independence study of the rectangular microchannel with aspect ratio one and  $\delta_{sf} = 1$  is done for five different mesh sizes of  $20 \times 20 \times 100$ ,  $24 \times 24 \times 600$ ,  $32 \times 32 \times 800$ ,  $40 \times 40 \times 1000$ ,  $48 \times 48 \times 1200$  at a Re of 100. The local Nusselt number and their relative errors were compared with the finest mesh size. The local Nusselt number varied by 5.906%, 3.876%, 1.202%, 0.768% on moving towards the finest grid. Relative error was less than 1% for the mesh no. 4. So, in order to have a unanimity between the computational time and accuracy, the intermediate mesh size of  $(40 \times 40 \times 1000)$  is selected for the simulation. Structured hexahedral elements in were considered for the simulation purpose.

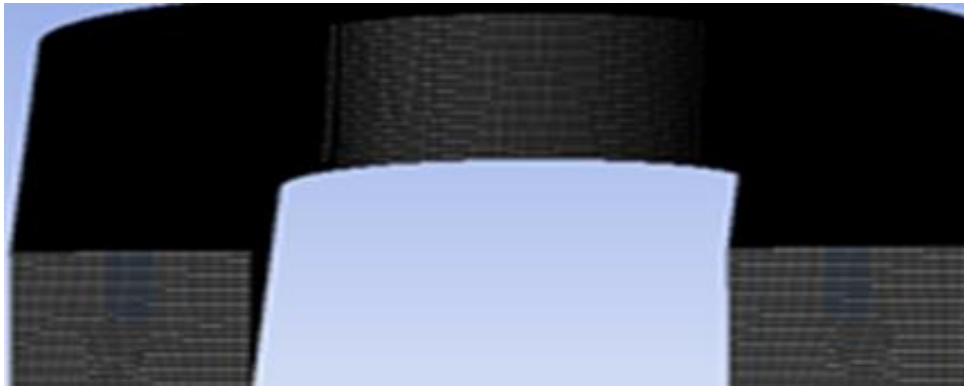


Figure 2: Structured mesh with quad elements of the U-bend section

### 3. MODEL VALIDATION

The present computational model is validated with available correlations to establish the correctness of the discretization scheme. Fig. 3 shows the variation of local Nusselt number ( $Nu_z$ ) with the existing correlation by Lee and Garimela [11] and Shah and London [12] and the friction factor results with the correlation of Steinke and Kandlikar [13]. It is observed from both the figures about the agreement of numerical model. Three different radius of curvature for the U bend section are considered and local variation of Nusselt number is analysed with varying Reynolds number for each case. It was observed that with an increase in radius of curvature of the U bend, the value of local Nusselt number increases sharply in the U bend section as shown which is compared with the SMC where there is no such sharp increase in . The increment in local Nusselt number extends to a greater length in case of  $R = 4$  mm because of which the maximum increase in  $Nu_{avg}$  was observed at  $R = 4$  mm. This is attributed to better mixing and flow recirculation at the U bend section. This paper used a computational method to analyze heat transfer through a 180 degree U-bend microchannel with a rectangular cross-section. Thermo-hydraulic performance is evaluated using the performance evaluation factor. The model employs a channel with a hydraulic diameter of 0.4 mm and three different radii of curvature  $r=2$ mm,  $r=3$ mm and  $r=4$ mm for three value of Reynolds numbers, 50, 100 and 200. Grid independence study of the rectangular microchannel with aspect ratio one is done for five different mesh sizes of  $20 \times 20 \times 100$ ,  $24 \times 24 \times 600$ ,  $32 \times 32 \times 800$ ,  $40 \times 40 \times 1000$ ,  $48 \times 48 \times 1200$  at a Re of 100. The local Nusselt number and their relative errors were compared with the finest mesh size. The local Nusselt number varied by 5.906 %, 3.876 %, 1.202 %, 0.768 % on moving towards the finest grid. Relative error was less than 1% for the mesh no.4. so, in order to have a unanimity between the computational time and accuracy, the intermediate mesh size of  $40 \times 40 \times 1000$  is selected for the simulation.

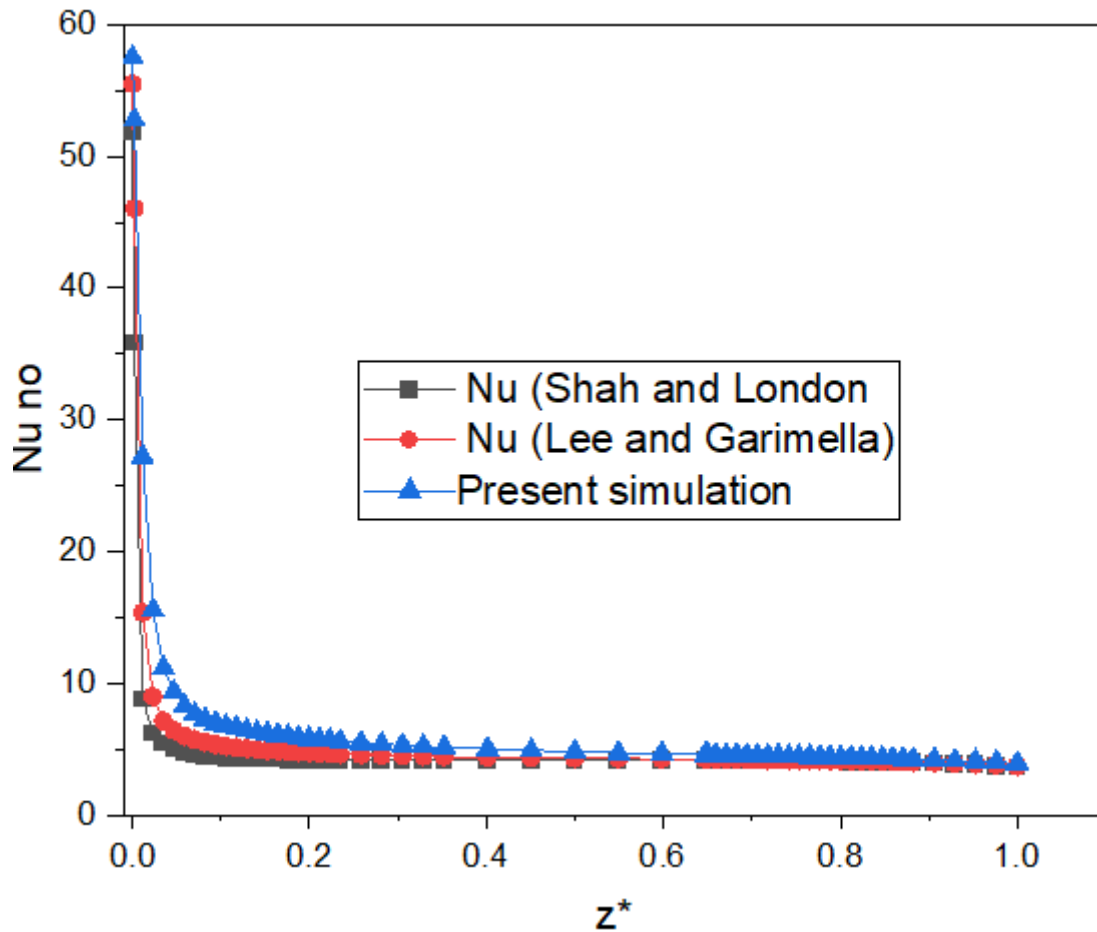


FIGURE 3: MODEL VALIDATION WITH (I) RESULTS FROM LEE AND Garimella [11], Shah and London [12] for local and fully developed Nusselt number and friction factor from results of Steinke and Kandlikar [13].

#### 4. RESULTS AND DISCUSSION

Effect of radius of curvature Three different radius of curvature for the U bend section are considered and local variation of Nusselt number is analysed with varying Reynolds number for each case. It was observed that with an increase in radius of curvature of the U bend, the value of local Nusselt number increases sharply in the The velocity profile in the laminar flow as shown below is disturbed due to the external centrifugal force and there is a shift in maximum velocity towards the concave channel wall because of which there is an increase in pressure also [6]. The pressure at a Re of 200 increases from 9.80% to 18 % when R changes from 3 to 4. Due to the redevelopment of thermal boundary layer in the bent section, there is an increase in heat transfer coefficient. As we move along the bend section of UBMC from at each 30° interval, the temperature is lower in the concave wall and the mass weighted average temperature in planes of bend portion is lower than the temperature in SMC corresponding to that particular. Now compare U- Bend microchannel (UBMC) with Straight microchannel (SMC) for same length that is if U-Bend microchannel is pull with inlet and outlet position then they formed straight microchannel. We consider R=4mm and Re=50 and for straight microchannel L=42.5

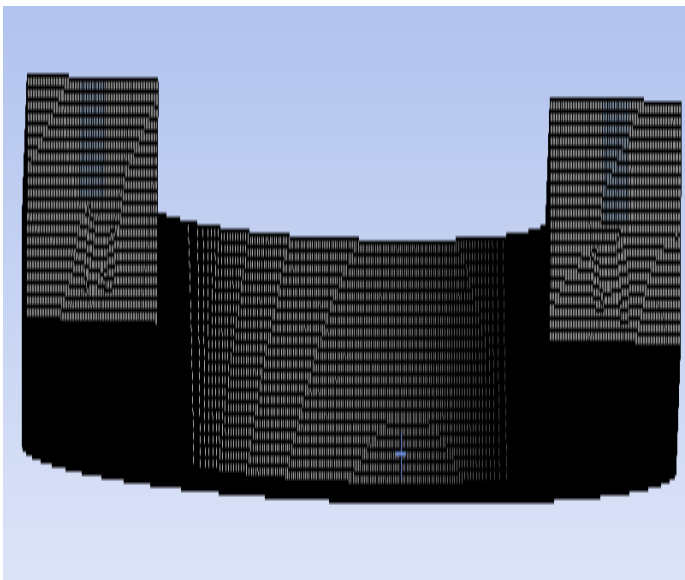


Fig no- 4 : Mesh for U – bend microchannel

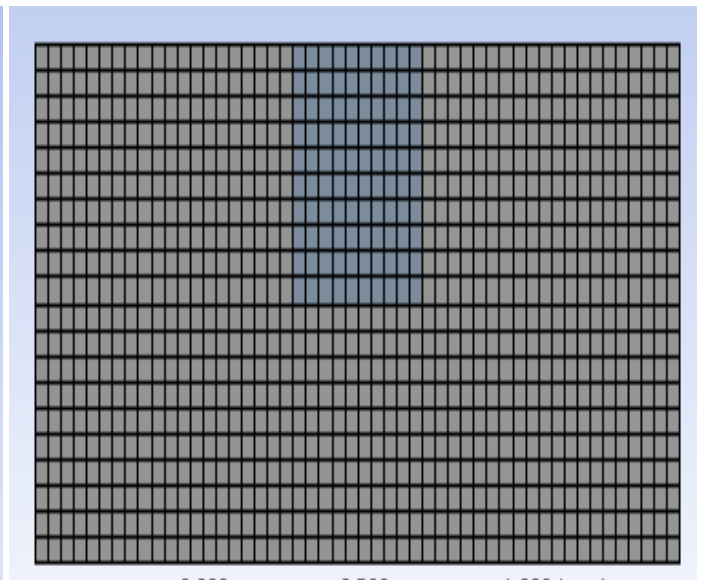


Fig no-5 : Mesh for straight microchannel

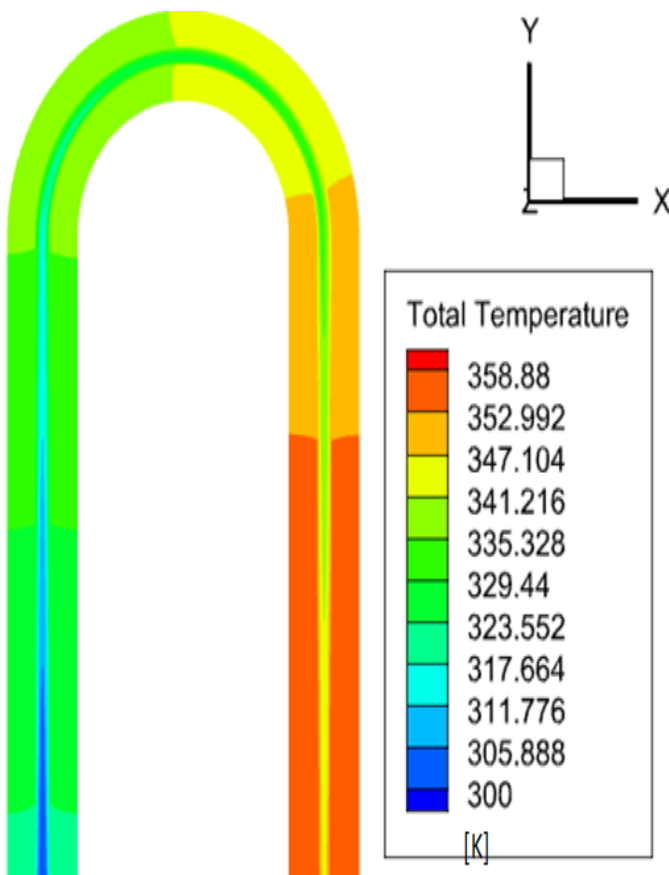


Fig no-6 Temperature contours of U B M C

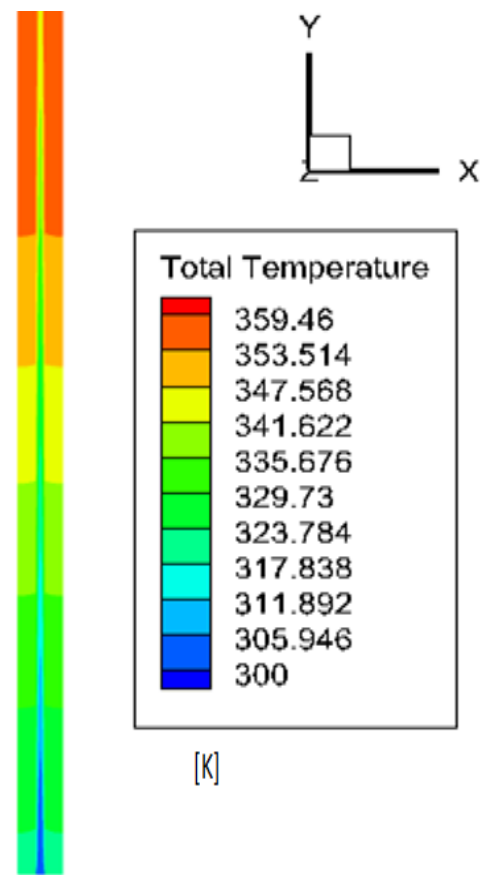


Fig no-7:Temperature contours of S M C

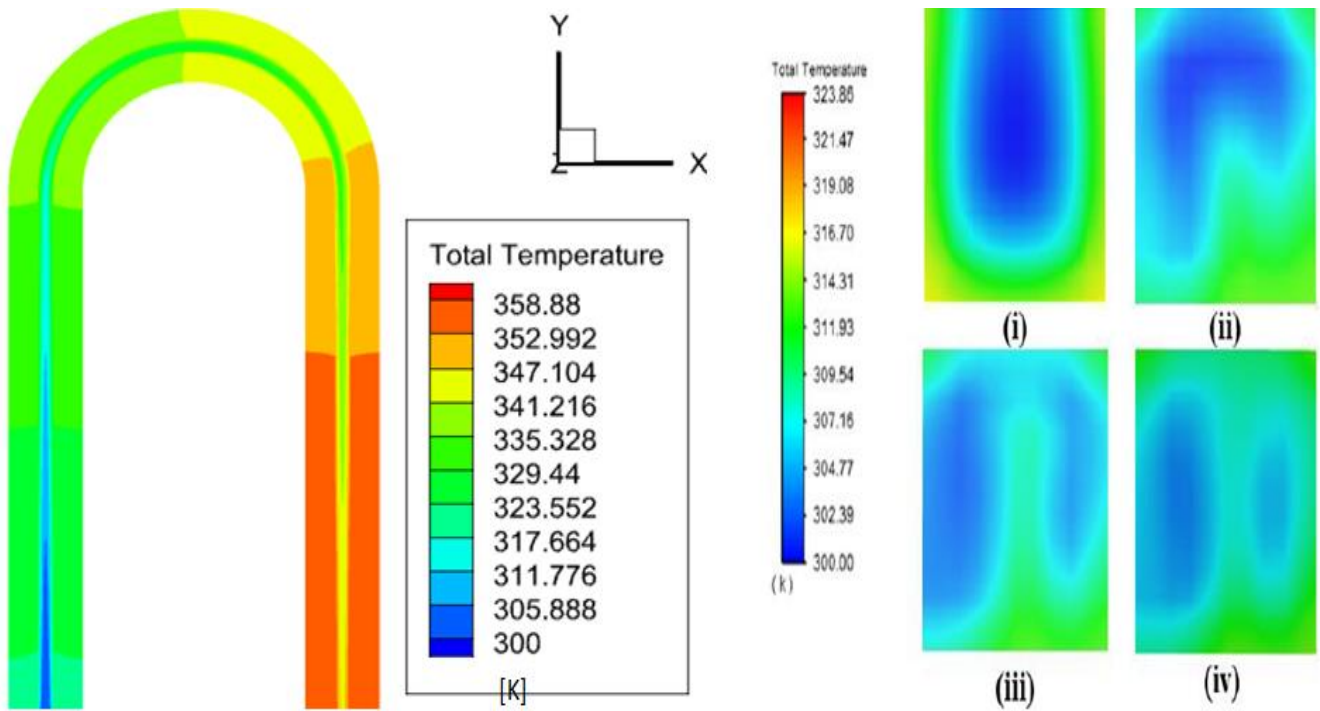


Fig no-8 : Temperature contour of UBMC in bend section at (i) 0° (ii) 30°, (iii) 60° and (iv) 90° from centre of the bend section for R = 4mm and Re =50

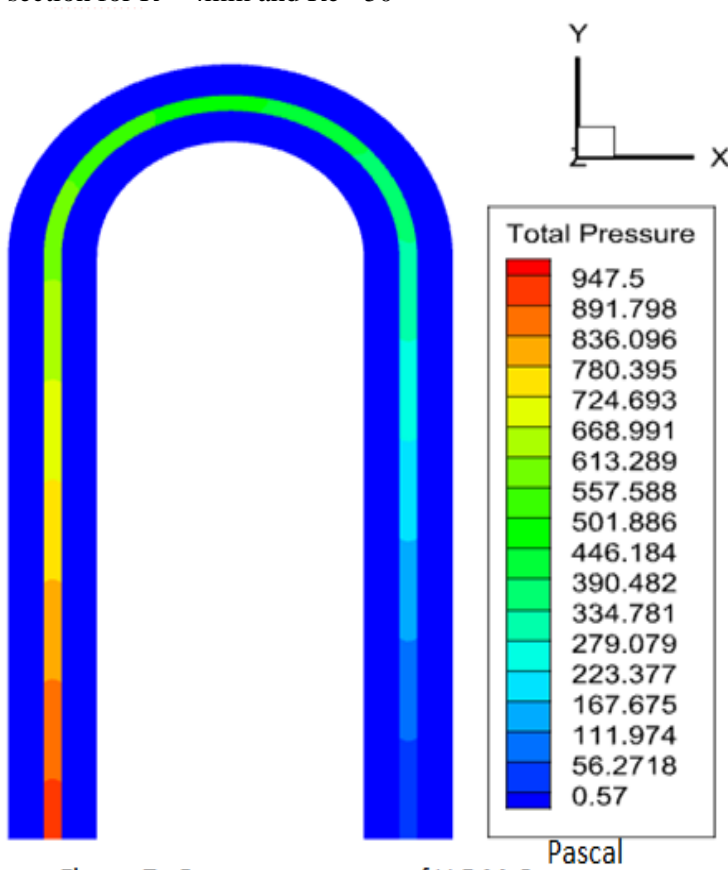


Fig no-9 : Pressure contours of U B M C

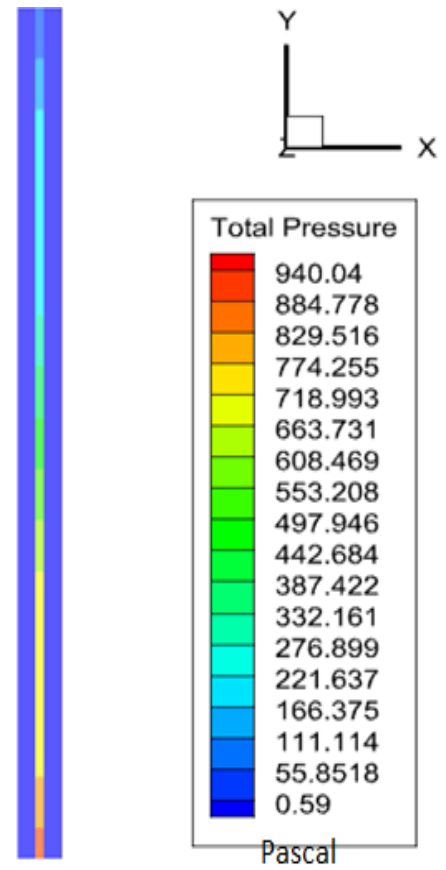


Fig no- 10 : Pressure contours of S M C

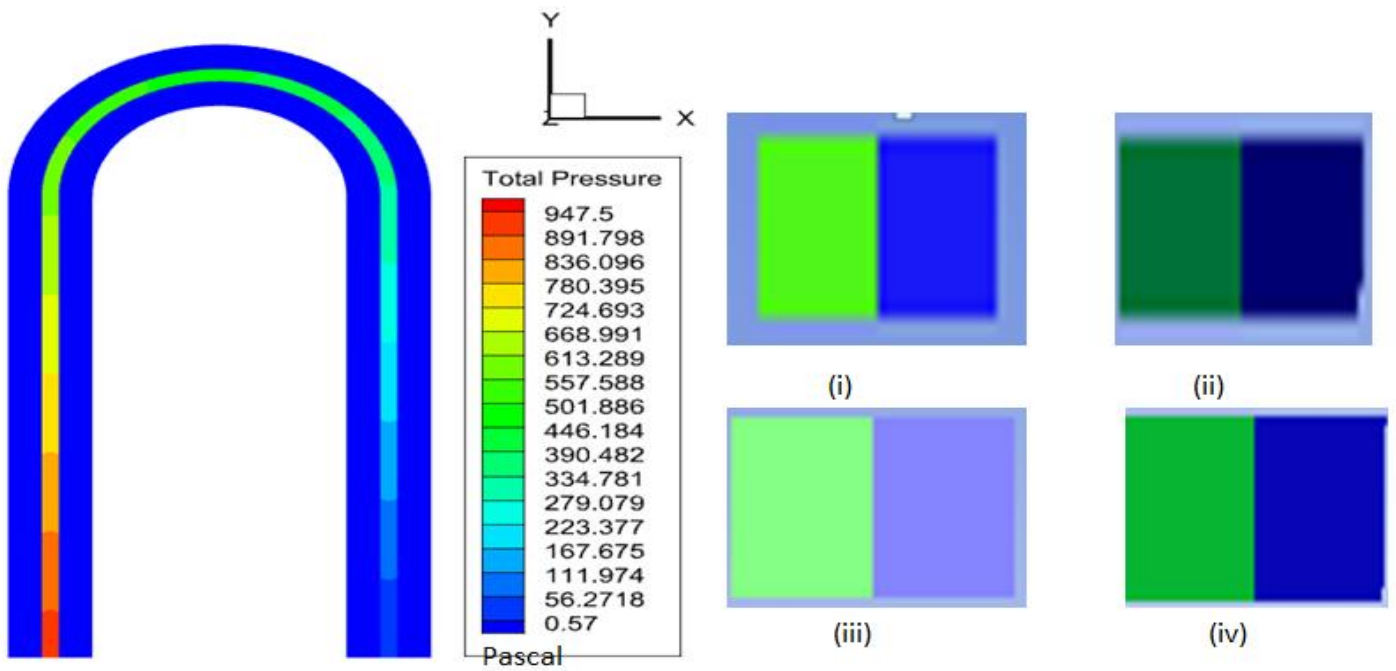


Fig no- 11 : Pressure contours of U B M C in bend section at (i) 0 (ii) 30°, (iii) 60° and (iv) 90° from centre of the bend section for R = 4mm and Re =50

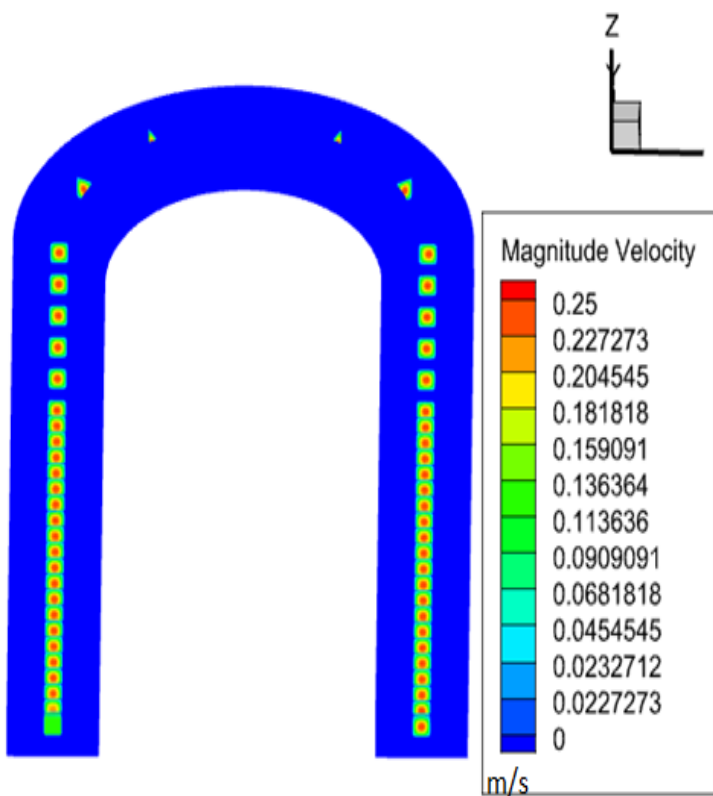


Fig no-12 : Velocity contours of U B M C

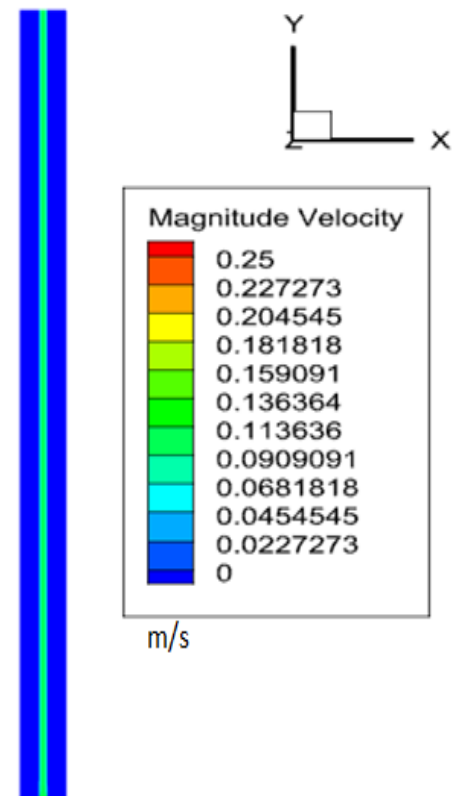


Fig no -13 : Velocity contour of S M C



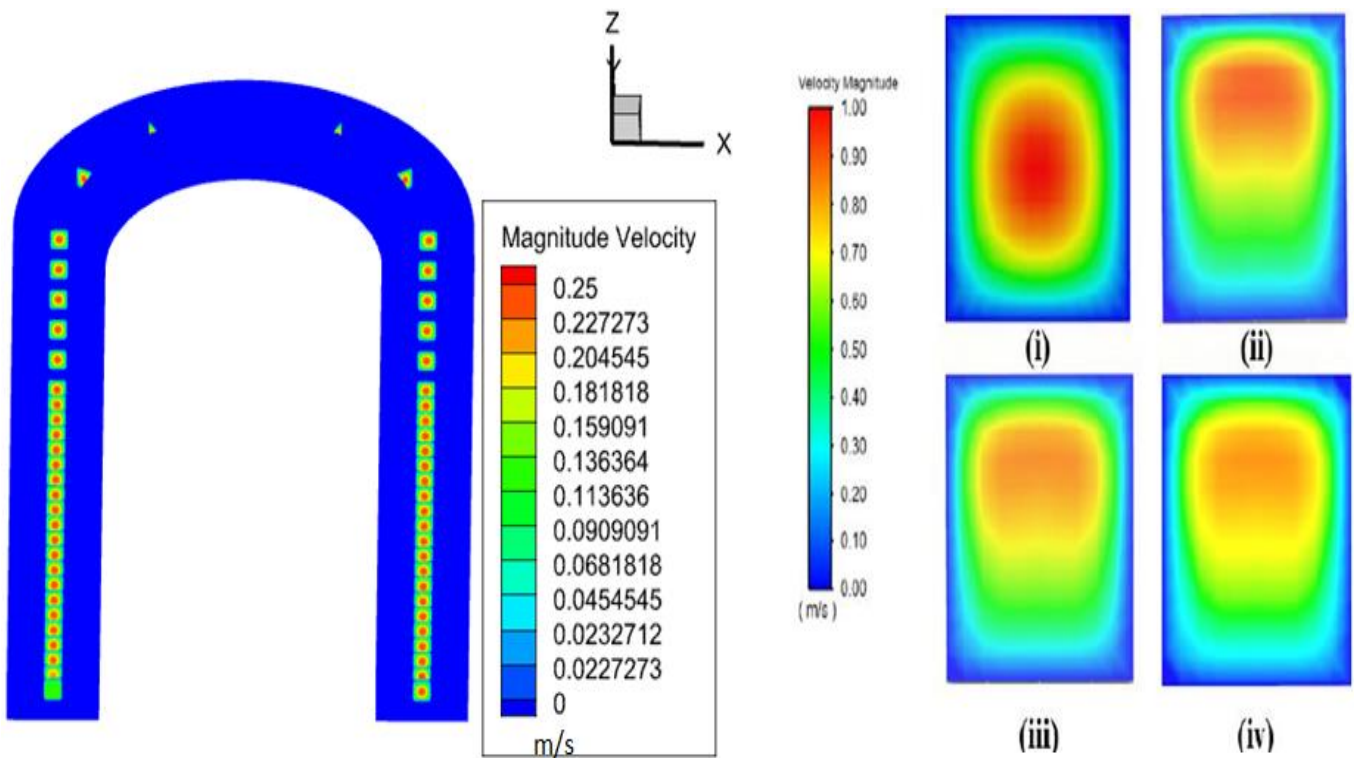


Fig no-14 : Velocity contour of UBMC in bend section at (i) 0° (ii) 30°, (iii) 60° and (iv) 90° from centre of the bend section for R = 4mm and Re =50

Axial variation of Nu no in UBMC and SMC.

where

$$Nu no = (h * Dh) / Kf$$

and

$$Z^* = Z / L$$

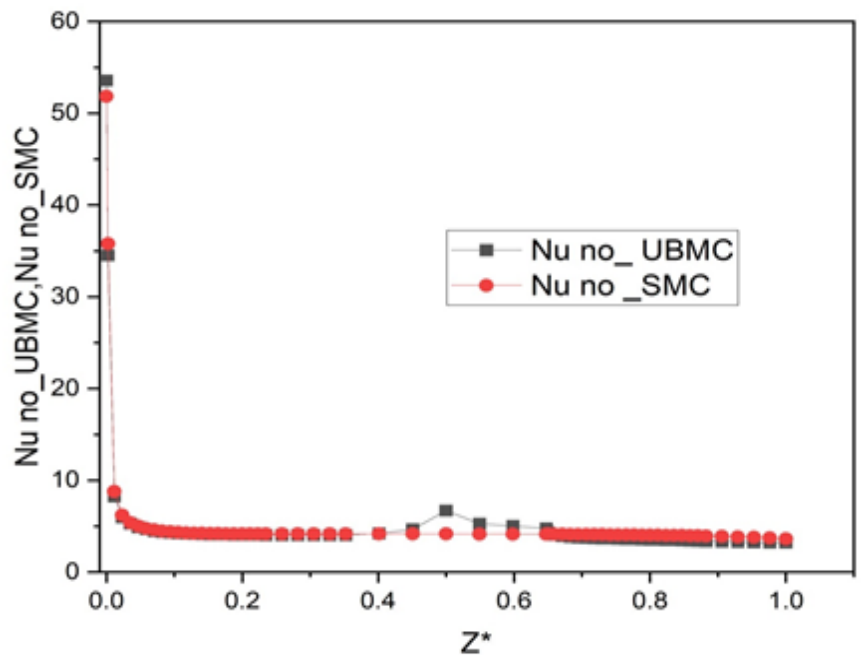


Fig no-15 :Graph between Nu no\_UBMC,Nu no\_SMC and Z\*

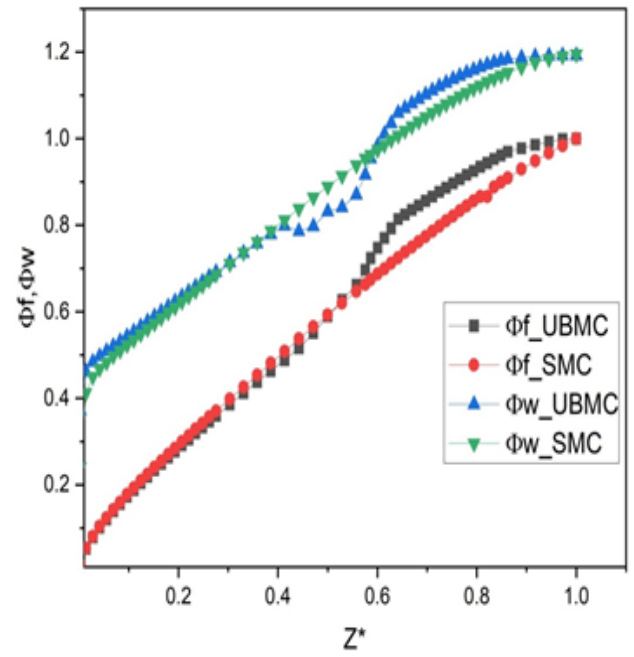
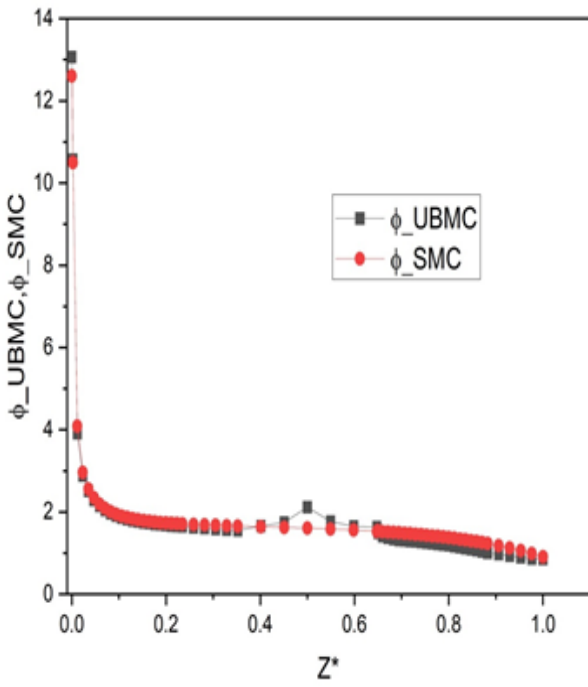


Fig no-16 :Graph between Phi\_UBMC,Phi\_SMC and  $Z^*$  , Fig no-17 :Graph b/w theta of fluid,wall and  $Z^*$

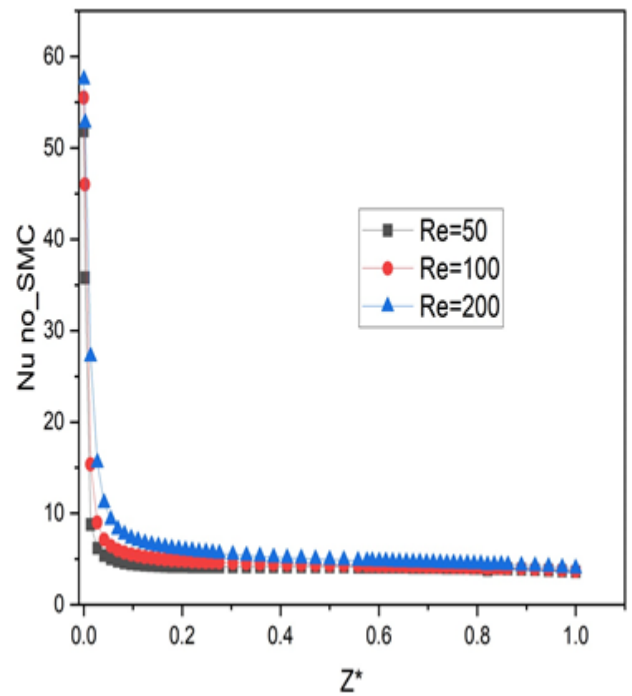
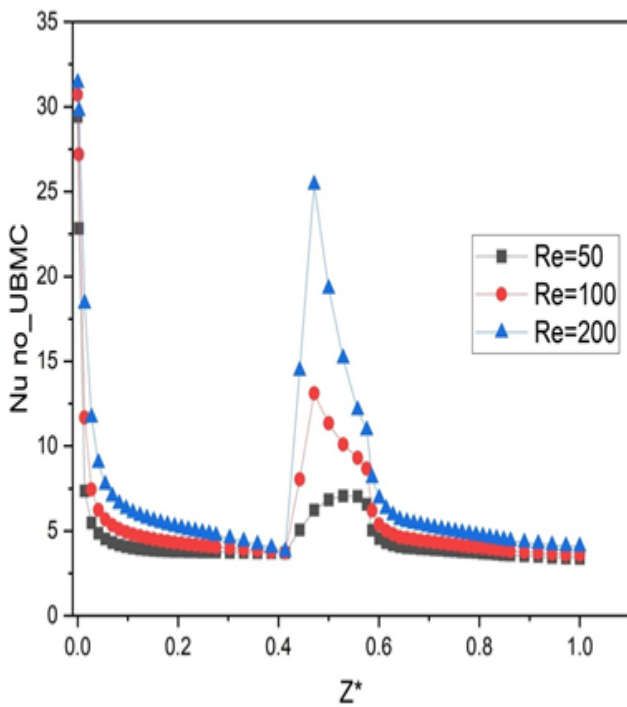


Fig no-18 :For UBMC , $R=2mm$  and  $Re=50,100,200$  UBMC, $R=2mm$  graph b/w  $Nu$  and  $Z^*$  for differ  $Re$  Fig no-19 : For SMC, $L=36.2mm$  and  $Re=50,100,200$  SMC, $L=36.2mm$  graph b/w  $Nu$  and  $Z^*$  for differ  $Re$

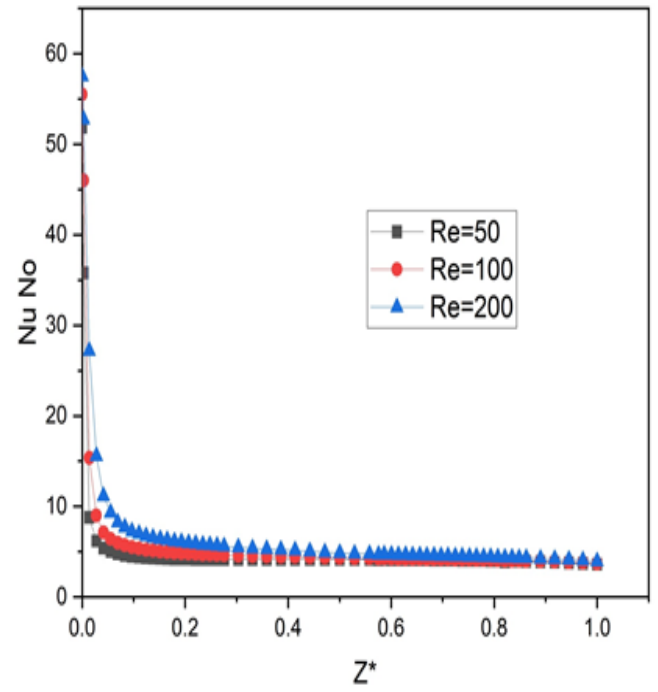
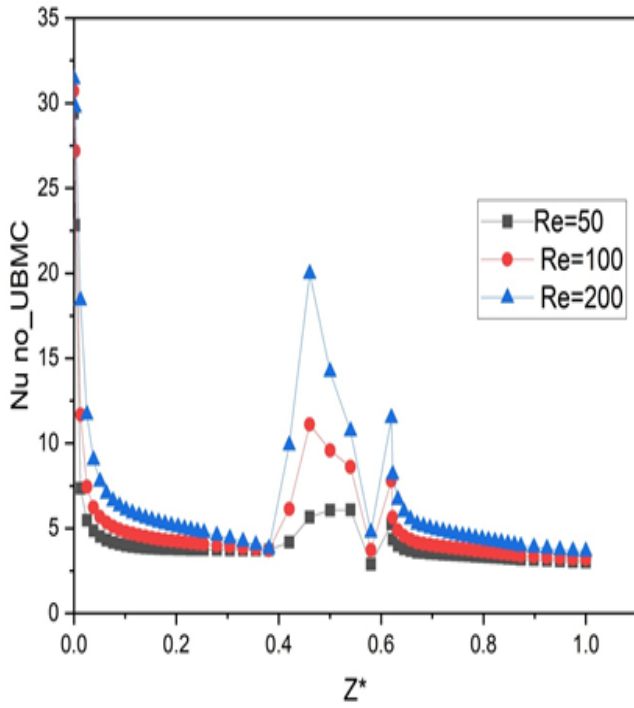


Fig no-20 :For UBMC ,R=3mm and Re=50,100,200 UBMC,R=3mm graph between Nu no and Z\*for different Re

Fig no-21 :For SMC,L=39.4mm and Re=50,100,200 SMC,L=39.4 mm graph between Nu no and Z\* for different Re

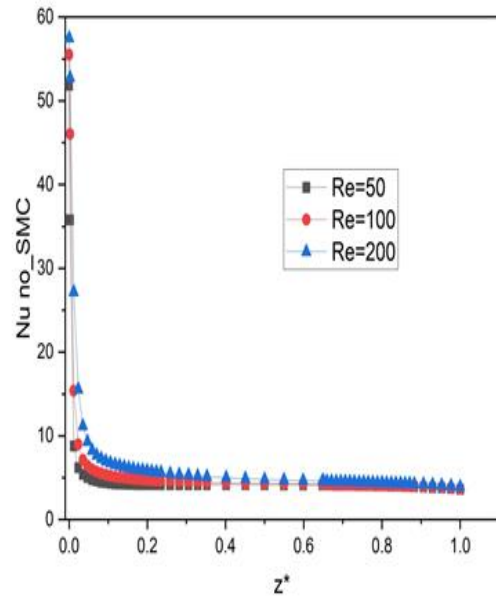
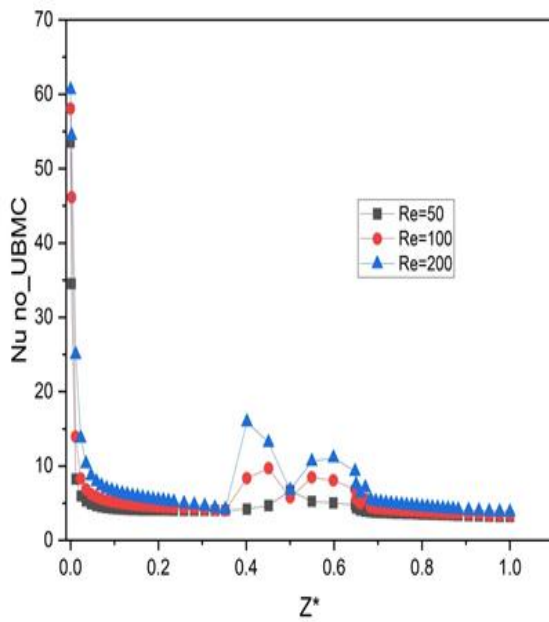


Fig no-22 :For UBMC ,R=4mm and Re=50,100,200 UBMC,R=4mm graph between Nu no and Z\*for different Re

Fig no-23:For SMC,L=42.5mm and Re=50,100,200 SMC,L=42.5mm graph between Nu no and Z\* for different Re no

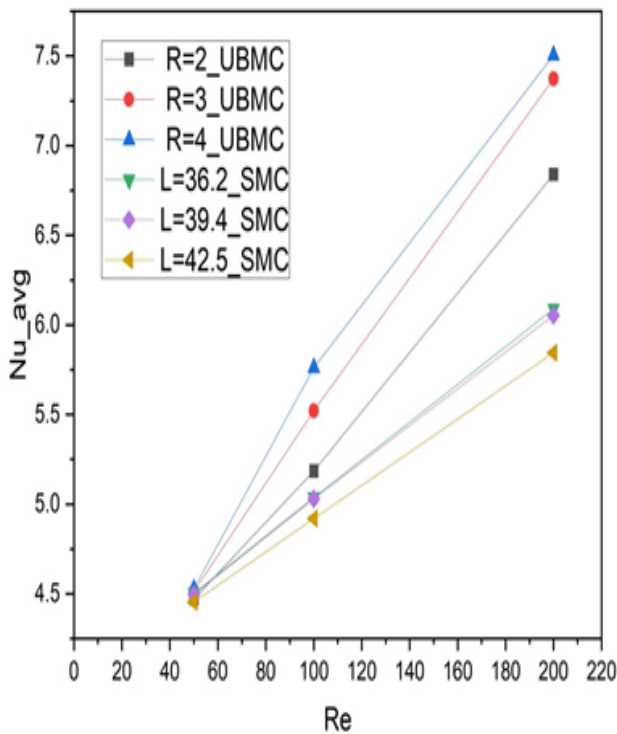


Fig no-24 : Average Nu no for UBMC and SMC Graph between average Nu no and Re no

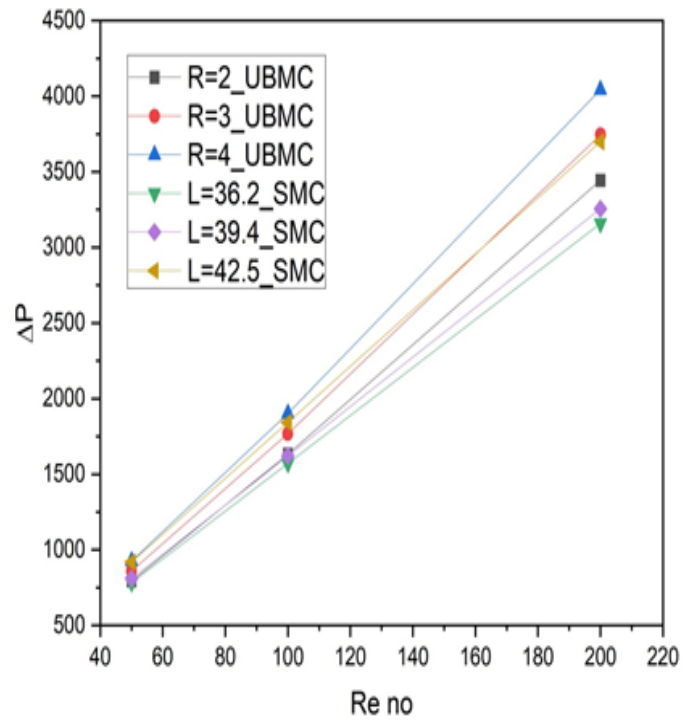


Fig no-25 : Pressure drop for UBMC and SMC Graph between pressure drop and Nu no and Re no

Performance Evaluation Factor(PEF)

$$PEF = \frac{Nu_{avg}/Nu_o}{(\Delta p/\Delta p_o)^{\frac{1}{2}}}$$

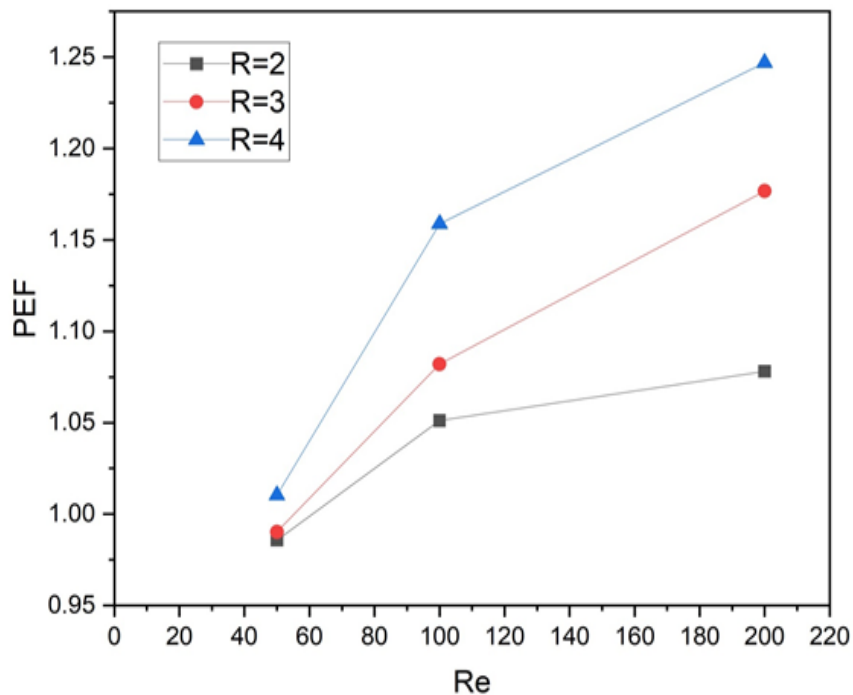


Fig no-26 : Graph between PEF and Re no

### 5. CONCLUSIONS

Heat transfer and fluid flow characteristics of a U-Bend microchannel (UBMC) is investigated through a numerical model that is capable to evaluate the performance of the proposed model compared to the simple and straight microchannel (SMC). The study was carried for different values of radius of curvature for the U-Bend section, R = 2 mm, 3 mm, 4mm with the corresponding length of SMC, L = 36.2mm,39.4mm, and 42.5 mm respectively. The effect of radius of curvature on the performance of UBMC is evaluated in terms of performance evaluation factor (PEF). Due to the presence of bend

there is an effect of centrifugal force because of which there is a shift in location maximum velocity due to the change in velocity profile. This induces extra pressure drop but there is an improvement in the rate of heat transfer also due to better mixing of fluid. This is quantified by the PEF that is greater than one for each parametric variation and there is up to 33% improvement in the thermo-hydrodynamic performance for  $R=4\text{mm}$  at a Reynolds number of 200. Performance of UBMC with low radius of curvature could be improved with high pumping power, since the pressure drop is unavoidable so it is better to use channels with high radii of curvature at relatively low Reynolds number or less pumping power. The effect of axial conduction needs investigation in order to predict the optimal value of Nusselt number. This will be addressed in future work.

## NOMENCLATURE

$A$	Area of cross-section	$[\text{m}^2]$
$C_p$	Specific heat at constant pressure	$[\text{J/kgK}]$
$D_h$	Hydraulic diameter	$[\text{m}]$
$h_z$	Local heat transfer coefficient	$[\text{W/m}^2\text{K}]$
$k_f$	Thermal conductivity of fluid	$[\text{W/mK}]$
$k_s$	Thermal conductivity of Solid	$[\text{W/mK}]$
$L$	Length of the substrate	$[\text{m}]$
$Nu_z$	Local Nusselt number	
$Nu_{avg}$	Average Nusselt number	
$p$	Pressure	$[\text{N/m}^2]$
$\Delta p$	Total pressure drop	$[\text{N/m}^2]$
$q''_{app}$	Applied heat flux	$[\text{W/m}^2]$
$Q$	Heat transfer rate	$[\text{W}]$
$Re$	Reynolds number	
$T$	Temperature	$[\text{K}]$
$T_f$	Fluid temperature	$[\text{K}]$
$T_s$	Solid temperature	$[\text{K}]$
$T_w$	Wall temperature	$[\text{K}]$
$z^*$	Non dimensional axial distance	
$W$	Total width	$[\text{m}]$
$W_s$	Width of solid substrate	$[\text{m}]$
$W_f$	Width of the fluid channel	$[\text{m}]$
$\mu$	Dynamic viscosity	$[\text{Ns/m}^2]$
$R$	Radius of curvature	$[\text{m}]$

## REFERENCES

- [1] Zhang, J. Lin, P. T, and Jaluria, Y (2011). Designs of multiple microchannel heat transfer systems, ASME International Mechanical Engineering Congress and Exposition (Vol.54976, pp 875-887).
- [2] Moharana, M. K., Singh, P.K, and Khandekar, S.(2012) optimum Nusselt number for simultaneously developing internal flow under conjugate conditions in a square microchannel, Journal of Heat Transfer,134(7).
- [3] Shah, R.K., and London, A.L,(2014).Laminar flow forced convection in ducts: a source book for compact heat exchanger analytical data. Academic press.
- [4] Nivedita , N .,Ligrani, P., and Papautsky, I .(2017).Dean flow dynamics in low –aspect ratio spiral microchannels, Scientific Reports,7(1),1-10.
- [5] Al-Neama,A.F.,Kapur,N .,Summers, J., and Thompson, H. M.(2017). An experimental and numerical investigation of the use of liquid flow in serpentine microchannels for microelectronics cooling, Applied Thermal Engineering, 116, 709-723.
- [6] Samal, S. K., and Moharana, M. K (2019). Thermohydraulic performance evaluation of a novel design recharging microchannel, International Journal of Thermal Sciences,135,459-470.
- [7] Pradhan, H.K., Sahoo, A.K., Roul, M. K., Awad, M.M., and Barik, A.K. (2020) Heat transfer characteristics of an 180 degree bend pipe of different cross sections using nanoenhanced ionic liquids(NELSS), SN Applied Sciences, 2(6),1-13.